

EXPERIMENTAL OBSERVATION OF SPACE CHARGE DRIVEN RESONANCES IN A LINAC

L. Groening, W. Barth, W. Bayer, G. Clemente, L. Dahl, P. Forck, P. Gerhard,
 I. Hofmann, M.S. Kaiser, M. Maier, S. Mickat, T. Milosic, H. Vormann,
 S. Yaramyshev, GSI, D-64291 Darmstadt, Germany
 D. Jeon, SNS, ORNL, Oak Ridge, TN 37831, USA
 D. Uriot, CEA IRFU, F-91191 Gif-sur-Yvette, France

Abstract

Recent experiments at the Universal Linear Accelerator (UNILAC) at GSI provided evidence for space charge driven resonances along a periodic DTL. A transverse fourth order resonance has been detected by recording the four fold symmetry in phase space. As predicted in [D. Jeon et al., Phys. Rev. ST Accel. Beams **12**, 054204 (2009)], the resonance dominates over the envelope instability. Additionally, evidence for resonant emittance transfer from the longitudinal to the transverse plane has been found for settings providing equal depressed phase advances of the involved planes.

TRANSVERSE RESONANCE

Transverse resonances are well known from circular machines even for very low beam current. Single devices create perturbing kicks to the particles passing the devices many times. Depending on the phase advance of the unperturbed particle oscillation, such kicks might cause resonant amplitude increase of the oscillation. In linacs each device is passed just once and single devices cannot cause resonant perturbation. For high currents the space charge force acts permanently on each particle. Its strength depends on the beam envelope size. Along periodic focusing channels the well matched envelope therefore acts as periodic perturbation to each beam particle. Since also linacs have periodic channels, such space charge driven resonances might occur also in linacs. Many particle simulations indeed predicted the occurrence of a 4th-order resonance along the DTL of GSI's Universal Linear Accelerator (UNILAC) at depressed transverse phase advances σ_{\perp} close to 90° [1]. Many features of space charge driven resonances can be understood from a simple particle-core model. A matched beam envelope with radial symmetry and breathing radius is assumed

$$R(s, \sigma_{env}) = R_o(\sigma_{env}) + \Delta R(\sigma_{env}) \cdot \cos(\sigma_{env}s), \quad (1)$$

where σ_{env} is the envelope phase advance. Its radial electric space charge field is

$$E_r = \frac{18 \cdot I}{\pi \epsilon_o \cdot R(s)^2 \beta c} \left[r - \frac{r^3}{2R(s)^2} + O(r) \right], \quad (2)$$

where I is the mean pulse current and β is the relative beam velocity. Each single particle is subject to the sum of external focusing with phase advance $\sigma_{\perp,o}$ and periodic space

charge force. Accordingly, its motion follows

$$r'' = -\sigma_{\perp,o}^2 r + \frac{e \cdot q}{A \cdot m_u} \cdot E_r \quad (3)$$

with the ion charge state q and total mass of $A \cdot m_u$. The equations can be merged to

$$r'' + \sigma_{\perp}^2 r \sim r^3 \cdot e^{i\sigma_{env}s} \quad (4)$$

being the equation of a disturbed oscillator with σ_{\perp} as depressed phase advance. Choosing the ansatz $r = C \cdot e^{-i\sigma_{\perp}s}$ for the disturbed oscillation leads to the resonance condition $\sigma_{env} = 4\sigma_{\perp}$. Since the phase advance of the matched envelope is 360°, the resonance occurs at $\sigma_{\perp} = 90^\circ$. Equations (1) to (3) can be integrated numerically for several initial single particle coordinates (r, r') . Fig. 1 shows the deformation of an initial distribution with the particles forming concentric ellipses. The initial distribution has been tracked through the first DTL tank of the UNILAC using a 7.1 mA beam of $^{40}\text{Ar}^{10+}$ at 1.4 MeV/u. The beam core is not affected since the perturbation scales with the third power, but outer beam particles are resonantly excited and the final phase space distribution features four wings attached to the beam core. These wings cause rms emittance growth. Direct observation of these wings proofs the occurrence of a 4th-order resonance.

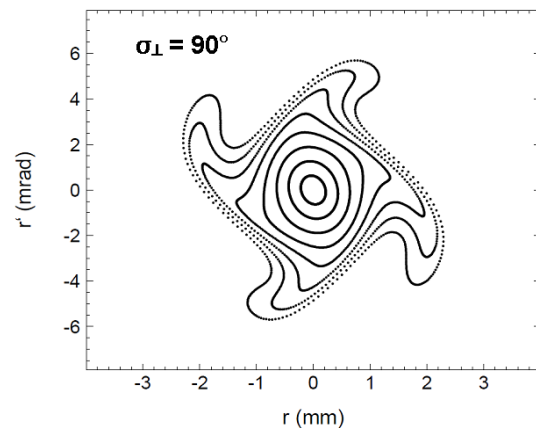


Figure 1: Distribution of particles at the exit of the periodic channel according to the radial particle-core model of the space charge driven transverse 4th-order resonance.

PARAMETRIC INTER-PLANE RESONANCE

Parametric resonances are collective effects and cannot be understood from particle-core models. In each plane i the beam temperature can be defined being proportional to the product $\epsilon_i \cdot \sigma_i$ of rms emittance and depressed phase advance. Temperature exchange, i.e. emittance transfer between longitudinal and transverse plane, can occur if $2\sigma_{\parallel} - 2\sigma_{\perp} = 0$, known as “resonant equipartitioning” [2, 3, 4]. Figure 2 displays the amount of expected emittance exchange (intensity of blue color) as a function of the depressed phase advances in the involved planes. Such Hofmann charts depend just on the rms emittance ratio and the presented chart has been calculated for a 7.1 mA beam of $^{40}\text{Ar}^{10+}$ at the entrance to the UNILAC Alvarez DTL. The longitudinal rms emittance is 10 times larger w.r.t. the transverse one. Generally in all modern hadron linacs the longitudinal emittance exceeds the transverse one. Avoiding parametric resonances has become a commonly applied design rule [5], although its validity has been never confirmed experimentally.

As for the transverse 4th-order space charge resonance, the minimization of mismatch is mandatory for the experimental observation of the parametric resonance. Despite resonances discussed here, envelope mismatch is the main cause of emittance dilution of space charge effected beams along periodic structures.

EXPERIMENTAL SET-UP AND PROCEDURE

The UNILAC at GSI [6] can accelerate all ion species from protons to uranium to an energy of up to 11.4 MeV/u. In order to cover the wide range of ion masses, the rf-field strengths and the magnetic quadrupole field strengths

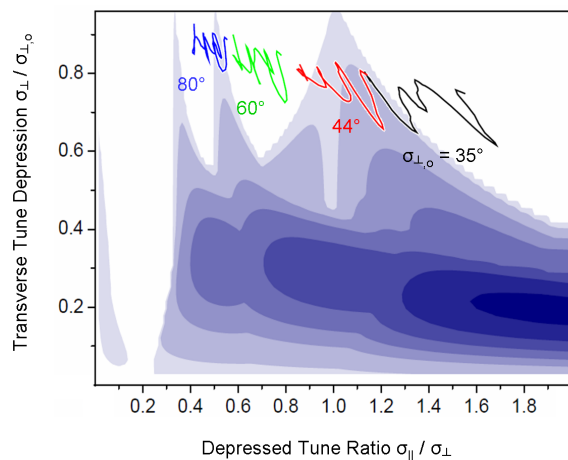


Figure 2: Hofmann chart for longitudinal to transverse emittance ratio of 10 and simulated paths of the depressed phase advances for transverse zero current phase advances of 35°, 44°, 60°, and 80°.

can be adjusted depending on which ion needs to be provided. For the ion $^{40}\text{Ar}^{10+}$ the full range of stable transverse zero current phase advances of up to 180° can be set. This operational flexibility requires enhanced availability of beam diagnostics devices compared with linacs that need to provide beams of one ion species only [7]. The experiment was carried out using the first tank of the UNILAC’s Alvarez-type DTL as shown schematically in Fig. 3. Along this tank ions are accelerated from 1.4 MeV/u to

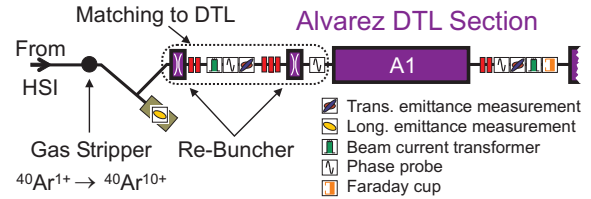


Figure 3: Schematic set-up of the experiments (not to scale).

3.6 MeV/u using an rf-frequency of 108 MHz. Longitudinal beam focusing is achieved by operating -30° from rf-crest, while transverse focusing uses a quadrupolar F-D-D-F lattice. The tank has 63 rf-gaps and each of the 62 drift tubes houses one quadrupole such that the DTL comprises 15 complete lattice cells. A dedicated matching section (Fig. 4) in front of the DTL is used for rms matched injection into its periodic lattice. Behind the DTL an additional slit/grid set-up for transverse emittance measurement and a beam transformer for beam transmission control were used. For the 7.1 mA $^{40}\text{Ar}^{10+}$ beam the transverse zero current phase advance $\sigma_{\perp,0}$ was varied from 35° to 130°, keeping the longitudinal zero current phase advance constant at 43°. Accordingly, the depressed phase advance ratio $\sigma_{\parallel}/\sigma_{\perp}$ was varied from 1.5 to 0.3.

As pointed out previously, mitigation of emittance growth from mismatch is mandatory. The periodic solution of the 3d-envelope with space charge inside the DTL is calculated numerically [8] using the results of transverse emittance measurements along the matching section (Fig. 4) as well as the rms bunch length measurements before the first re-buncher of this section. The procedure to obtain the rms Twiss parameters at the section’s entrance is described in [9]. Using this parameters at the entrance to the section as initial condition for rms envelope tracking with linear space charge forces [10], the final rms parameters at the DTL entrance depend on the strengths f_n of the seven focusing elements of the section. The final rms parameters together with the periodic solution define the mismatch M_i in each plane [11]. Matched injection is achieved if all M_i vanish. The settings f_n that minimize all M_i simultaneously are determined numerically. Additionally, the achieved mismatch was estimated by simulations with the DYNAMION code [12] using 3d-particle-particle interaction. The result is shown in Fig. 5 plotting the mismatch in each plane as a function of the transverse phase advances applied during the measurements. Residual mismatch is due

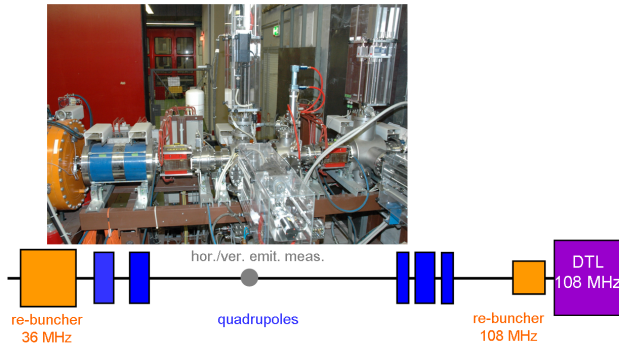


Figure 4: Matching section to the DTL comprising two re-bunchers, five quadrupoles, and a transverse slit/grid emittance measurement unit.

to bucket overflow (longitudinal) and to rf-curvature and nonlinear space charge forces along the matching section (transverse).

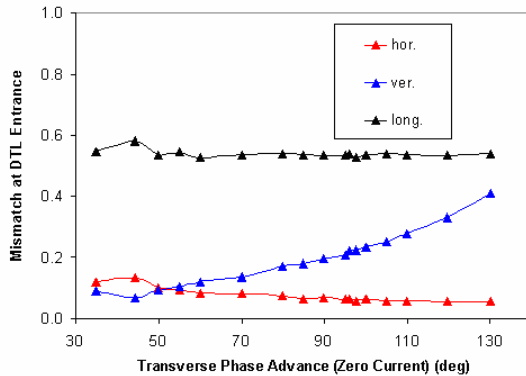


Figure 5: Mismatch factors in the three planes at the DTL entrance as obtained from DYNAMION simulations. The definition of mismatch is taken from [11].

RESULTS FROM MEASUREMENTS

4th-order Transverse Resonance $\sigma_{\perp} = 90^{\circ}$

The 4th-order transverse resonance is expected close to the depressed transverse phase advance σ_{\perp} of 90° . To estimate the impact of the envelope instability, transverse rms beam sizes delivered by the DYNAMION code have been evaluated along the beam line. Figure 6 plots the horizontal beam width for three different phase advances. Also for $\sigma_{\perp,o} = 120^{\circ}$ no envelope instability is observed. The envelope ripple at 100° is driven by the 4th-order resonance. Additionally, during the preparation of the experiments, simulations using a KV-distribution of 5000 particles with similar rms emittances and equal mismatch to the DTL have been done. The simulations revealed very low emittance growth of less than 10%. KV-distributions do not have a 4th-order space charge potential term and the small growth is from an artificial 4th-order potential term

04 Extreme Beams, Sources and Other Technologies

4D Beam Dynamics, Computer Simulation, Beam Transport

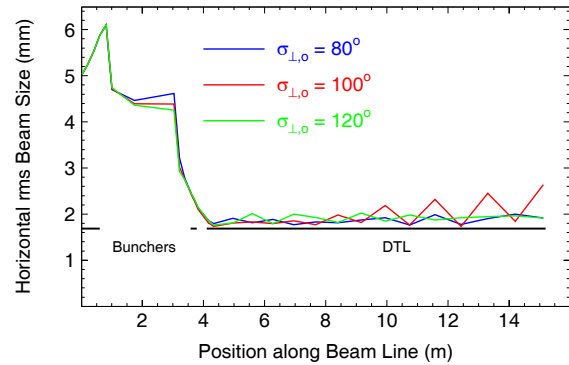


Figure 6: Horizontal rms beam envelope along the beam line for three different transverse phase advances as simulated with DYNAMION.

driven by numerical noise from the finite number of particles being used.

For phase advances $\sigma_{\perp,o}$ from 60° to 130° , measured and simulated transverse phase space distributions at the DTL exit are plotted in Fig. 7. The mean value of the horizontal and vertical rms emittance, i.e. $\epsilon_{rms,\perp} = (\epsilon_{rms,x} + \epsilon_{rms,y})/2$, is also presented in Fig. 7 as a function of the phase advance $\sigma_{\perp,o}$. The emittance $\epsilon_{rms,\perp}$ at the DTL exit was found to be independent of the phase advance for values of $\sigma_{\perp,o} \leq 90^{\circ}$. Growth was observed for $\sigma_{\perp,o} \geq 90^{\circ}$ in both transverse planes. These observations are in very good agreement to simulations done with three different codes, i.e. DYNAMION, PARMILA [13], and TRACEWIN [14]. The measured growth rate of $\epsilon_{rms,\perp}$ is constant for $\sigma_{\perp,o} \geq 110^{\circ}$. In the horizontal plane the measured growth disappeared for $\sigma_{\perp,o} \geq 110^{\circ}$ while the vertical growth increased, leading to a constant growth of the mean transverse emittance $\epsilon_{rms,\perp}$. Distributions corresponding to phase advances far away from the stop-band have elliptical shapes. At $\sigma_{\perp,o} \approx 100^{\circ}$ instead the measurements and the simulations clearly revealed four wings, which are typical for a resonant 4th-order interaction – here due to space charge. The experiments together with the KV-simulations demonstrated that the 4th-order resonance dominates over the envelope instability. This is in full agreement with the prediction of [1]. It seems that 15 periodic cells are too few to develop the envelope instability sufficiently strong, to be distinguished from the 4th-order space charge resonance. More details on the measurements of this resonance are given in [15].

Parametric Resonance $\sigma_{\perp} = \sigma_{\parallel}$

The parametric resonance is expected at equal depressed phase advances in the longitudinal and transverse plane. Figure 2 plots the paths of the phase advances along the stability chart for DTL settings of $\sigma_{\perp,o}$ from 35° to 80° . For $\sigma_{\perp,o} = 44^{\circ}$ the stop-band of equipartitioning is fully crossed. Figure 8 plots $\epsilon_{rms,\perp}$ measured at the DTL exit as a function of the depressed phase advance ratio $\eta = \sigma_{\parallel}/\sigma_{\perp}$

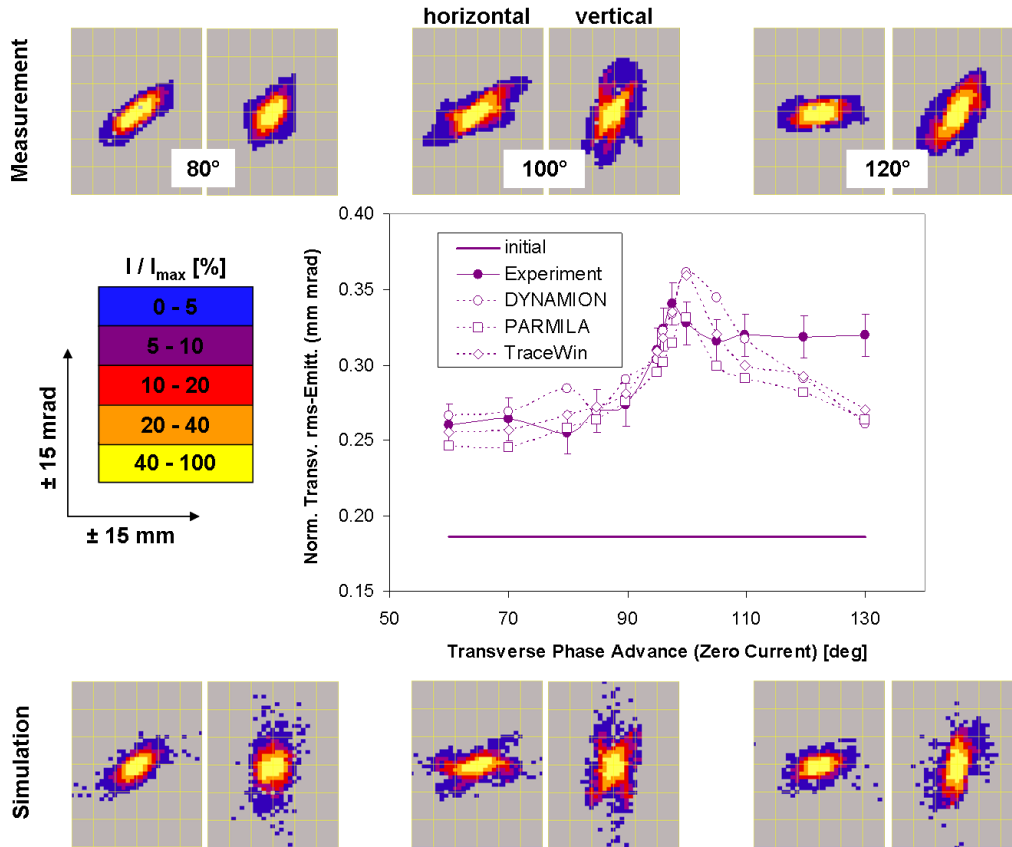


Figure 7: Upper and lower: phase space distributions at the exit of the first DTL tank as obtained from measurements and from the DYNAMION code for phase advances $\sigma_{\perp,o}$ of 80°, 100°, and 120°. Left (right) side distributions refer the horizontal (vertical) plane. The scale is ± 15 mm and ± 15 mrad. Fractional intensities refer to the phase space element including the highest intensity. Center: Mean of horizontal and vertical normalized rms emittance behind the first DTL tank as a function of the transverse zero current phase advance.

at the entrance to the DTL. For $\eta \leq 0.8$ a constant value of the transverse rms emittance has been measured. As η approaches 1.0 from below, considerable transverse emittance growth by about 20% w.r.t. the values measured for

$\eta \leq 0.8$ is observed. For $\eta \rightarrow 1.5$ the measured emittance shows a further increase not explained by the stability chart, while simulation indicates a slight increase. This experimental result is in good agreement with beam dynamics simulations performed with DYNAMION and TRACEWIN. Experimental data and simulations agree well on the overall dependence of the emittance on the phase advance ratio as well as on the absolute values. They also reflect the presence of the main stop-band within the stability chart (Fig. 2). For this reason we attribute the observed transverse emittance growth at $\sigma_{\parallel} \approx \sigma_{\perp}$ to resonant emittance exchange from the longitudinal plane to the transverse plane. Accordingly, the longitudinal rms emittance should shrink for the resonance case.

The limited space behind the DTL tank did not allow for measurements of the longitudinal phase space distribution. Additionally, for intense argon beams the UNILAC's total longitudinal emittance at the DTL entrance exceeds the area of the rf-bucket. The unavoidable rf-bucket overflow causes longitudinal rms emittance growth during acceleration. This growth is expected to mitigate the longitudinal emittance shrinking driven by emittance exchange. As the sum of emittances is expected to be constant [4] the rela-

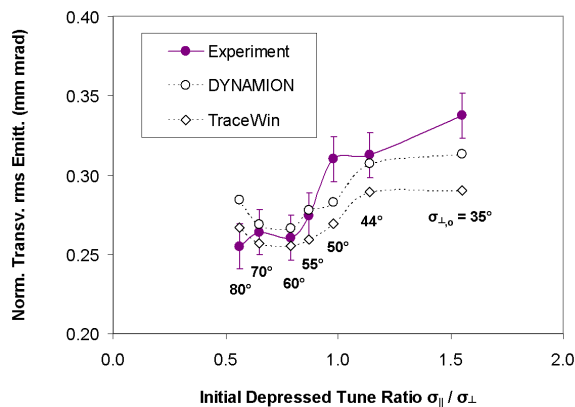


Figure 8: Mean of horizontal and vertical rms emittance at the DTL exit as a function of the initial ratio of depressed longitudinal and transverse phase advance.

tive longitudinal decrease from this source cannot exceed 2%, which would be hard to measure in any case. We have therefore evaluated the particle current confined within the ellipse having the size of the rms emittance at the DTL entrance. This evaluation has been done for each plane separately. To obtain a meaningful value for the current within a given ellipse area, the ellipse parameters β and α as well as the ellipse center must be chosen such that the confined number of particles is at maximum. The amount of particles within this ellipses is a measure for the phase space density within the distribution core. This amount has been evaluated along the beam line and it is plotted in Fig. 9. In the simulations the DTL was prolonged virtually in order to prolong the emittance exchange effect as shown by the dotted lines in Fig. 9. Comparison of the longitudinal

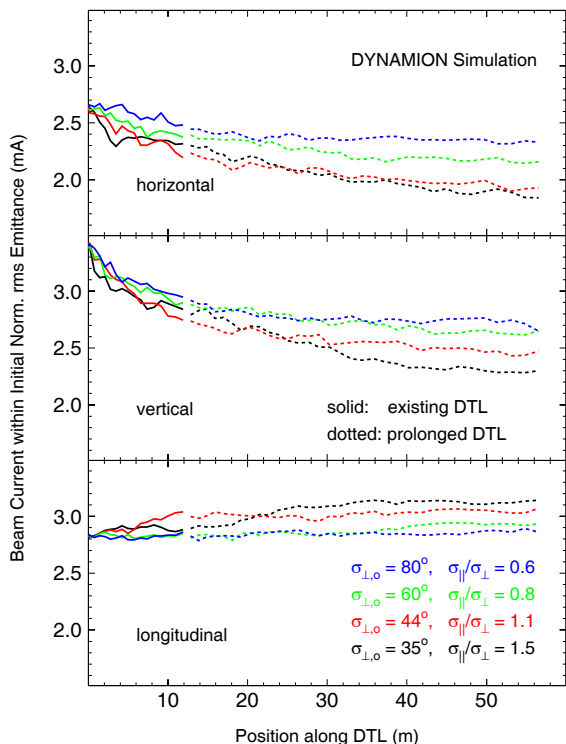


Figure 9: Beam current within the initial rms emittance as a function of position using the DYNAMION code. Solid lines correspond to the DTL used for the measurements, while dotted lines indicate results corresponding to a virtually prolonged DTL.

curves for the cases of $\eta=1.5$ and for $\eta=1.1$ indicates that the density increase for $\eta=1.5$ sets in at a later time with respect to the increase for $\eta=1.1$. This delay follows directly from the paths within the stability chart showing that the beam related to $\eta=1.5$ enters the resonance later with respect to the beam related to $\eta=1.1$. Core densities at the end of the DTL are plotted in Fig. 10 as a function of the phase advance ratio η at the DTL entrance. The final transverse core density generally decreases as η approaches 1.0, where it shows a minimum. The longitudinal density shows the complementary behavior, i.e. a maximum for $\sigma_{\parallel} \approx \sigma_{\perp}$.

04 Extreme Beams, Sources and Other Technologies

4D Beam Dynamics, Computer Simulation, Beam Transport

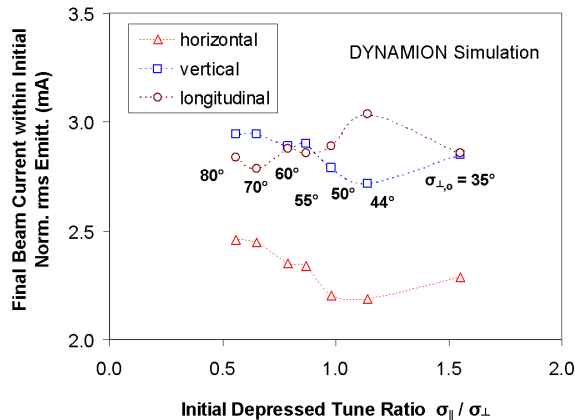


Figure 10: Simulated beam currents within the initial rms emittance at the DTL exit as a function of the initial ratio of depressed longitudinal and transverse phase advance.

In summary, we conclude that the experimental observations jointly with the results from simulations provide evidence for the existence of resonant emittance exchange along a high intensity linacs. Good agreement was found with the predictions from the theoretical stability charts, which are thus experimentally benchmarked as valid design tool. Reference [16] has more details on the campaign on the parametric resonance.

REFERENCES

- [1] D. Jeon et al., Phys. Rev. ST Accel. Beams **12**, 054204 (2009).
- [2] R.A. Jameson, AIP Conf. Proc. No. 279, p. 969.
- [3] I. Hofmann and O. Boine-Frankenheim, Phys. Rev. Lett. **87**, 034802 (2001).
- [4] I. Hofmann et al., Phys. Rev. ST Accel. Beams **6**, 024202 (2003).
- [5] T.P. Wangler, *Rf Linear Accelerators*, (2nd Ed. Wiley-VCH, Weinheim, 2008), p. 319.
- [6] W. Barth et al., Proc. of XXII Linac Conf., (2004).
- [7] P. Forck et al., Proc. of the XX Linac Conf., Monterey, U.S.A., (2000).
- [8] L. Groening et al., Proc. of 10th ICAP Conf. (2009).
- [9] L. Groening et al., Phys. Rev. ST Accel. Beams **11**, 094201 (2008).
- [10] see Ref. [5], p. 299.
- [11] see Ref. [5], p. 223.
- [12] S. Yaramyshev et al., NIM A **558**, 90 (2006).
- [13] J.H. Billen and H. Takeda, PARMILA Manual, Report LAUR-98-4478, Los Alamos, 1998 (Revised 2004).
- [14] <http://irfu.cea.fr/Sacm/logiciels/index.php>.
- [15] L. Groening et al., Phys. Rev. Lett. **102**, 234801 (2009).
- [16] L. Groening et al., Phys. Rev. Lett. **103**, 224801 (2009).